## RESEARCH

# Linkage of pipeline blockage to coagulation-flocculation process: effect of anionic polymer and pH

Rosalina Eka Praptiwi[1], Jyun-Cyuan Syu[1], Hai-Hsuan Cheng[1], Tsung-Hsiung Yu[2], Yu-Charng Wu[2] and Liang-Ming Whang[1,3*]

## Abstract

This study investigated the frequent blockages observed in the discharge pipeline in the chemical mechanical polishing wastewater treatment plant. Preliminary analyses indicated that blockages were predominantly consisted of residual organically-bounded Al due to overdosage of polyaluminum chloride (PACl) and anionic polymer during coagulation-flocculation process. To minimize the recurrence of blockage, jar test experiments were conducted in this study to identify optimum dosages of PACl and anionic polymer as well as optimum pH value. According to the model derived from jar tests, the optimum PACl dosage was dependent on the soluble Cu concentration of wastewater with low initial turbidity [< 1000 nephelometry turbidity units (NTU)]. The PACl dosage would require more than 5 mg L$^{-1}$ when soluble copper below 20 mg L$^{-1}$, while PACl is not necessary when more than 20 mg L$^{-1}$ of soluble copper in the wastewater. On the other hand, optimal PACl dosage was dependent on the initial turbidity of wastewater with high initial turbidity (> 1000 NTU), while the optimal PACl dosage was 30 mg L$^{-1}$ when initial turbidity around 7000 NTU. The change of pH in the range of 8 to 9.5 did not significantly affect the turbidity or Cu removal, however, higher pH increased the deposition of residual monomeric Al species which might lead to blockage. In summary, controlling PACl dosage at optimum dosage under the conditions of pH 8.5 ± 0.5 and 1 mg L$^{-1}$ polymer could reduce the blockage occurrence as well as maintain the effluent quality to meet the standards.

**Keywords:** Pipeline blockage, Polyaluminum chloride, pH, Anionic polymer

## 1 Introduction

Coagulation-flocculation using polyaluminum chloride (PACl) has been widely applied to treat semiconductor wastewater, particularly the waste stream from the chemical–mechanical polishing (CMP) process. The slurry used in CMP process typically consists of ultrapure water, abrasive materials such as silica ($SiO_2$), alumina ($Al_2O_3$), and ceria ($CeO_2$), and some additives like oxidizers, complexing agents,

corrosion inhibitors, etc. [1]. Accordingly, the CMP wastewater contains a high proportion of total solids, Si, and Cu with a relatively basic pH and negative zeta potential [2–4], in which Cu is from the fabrication of Cu metallization [5]. Compared to conventional aluminum salts, PACl was proved to have better efficiency in removing colloidal-Si [6–8]. Moreover, PACl has advantages, such as a broader range of optimum pH from 7 to 10 [9] and could generate stronger flocs [10]. The coagulation efficiency of PACl is associated with the highly positively charged polymeric Al species ($AlO_4Al_{12}(OH)_{24}(H_2O)_{12}^{7+}$ known as $Al_{13}$, and $Al_{30}O_8(OH)_{56}(H_2O)_{24}^{15+}$ known as $Al_{30}$), which provide
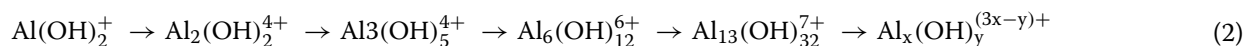
*Correspondence: whang@mail.ncku.edu.tw

[3] Sustainable Environment Research Laboratory, National Cheng Kung University, Tainan 701, Taiwan
Full list of author information is available at the end of the article

charge neutralization, electrostatic patch, and bridging [11, 12]. The hydrolysis of Al salts dissolved in aqueous solutions can be described as follows [13]:

$$Al^{3+} \leftrightarrow Al(OH)_2^+ \leftrightarrow Al(OH)^{2+} \leftrightarrow Al(OH)_3^0 \leftrightarrow Al(OH)_{3(am)} \leftrightarrow Al(OH)_4^- \tag{1}$$

$$Al(OH)_2^+ \rightarrow Al_2(OH)_2^{4+} \rightarrow Al3(OH)_5^{4+} \rightarrow Al_6(OH)_{12}^{6+} \rightarrow Al_{13}(OH)_{32}^{7+} \rightarrow Al_x(OH)_y^{(3x-y)+} \tag{2}$$

In order to enhance the coagulation-flocculation performance, the use of PACl has been coupled with polymer, which promotes bigger and stronger floc formation by adsorption-bridging [14].

In most of the existing industrial wastewater treatment plants in Taiwan, the coagulant and/or flocculant are overly dosed at constant rate to ensure turbidity removal and to reduce operational difficulty. Consequently, the residual coagulants and flocculants could cause blockages in the discharge pipeline by postprecipitation when flow velocity lower than the self-cleaning velocity [15]. In the case of minor blockages, an increase in pumping rate is needed to compensate for the reduction of the total available head [16]. When the blockages become severe, measures such as water jetting or pipeline replacement are necessary, leading to additional maintenance costs and possibly temporary shutdown. Moreover, effluent and blockage interaction in the discharge pipeline might worsen the water quality affecting its compliance to the permissible limit. In the case, it is imperative to continuously maintain optimum conditions in the coagulation-flocculation process to prevent blockages from recurring, while it was proposed that turbidity, streaming current, and conductivity could be the indicator for adjusting coagulant dosage automatically [17–19]. Furthermore, optimization of coagulation conditions could also be modeled using mathematical approaches such as polynomial response models, explaining the relationship among variables [20], although previous researches focused only on narrow ranges of water qualities including turbidity, conductivity, Cu and so on.

This study therefore aimed to optimize PACl dosage, polymer dosage, and pH, along with investigating the deposition behavior of residual metals (Al and Cu). Blockage samples collected from two CMP wastewater treatment plants were analyzed using scanning electron microscopy with energy dispersive X-rays (SEM/EDX). PACl, polymer, and pH were optimized using jar tests, and the deposition behavior of residual metals was investigated using in-bottle tests. Polynomial response models were derived to determine the relationship

between the possible indicators (turbidity, zeta potential, pH, and conductivity) with the independent variables (PACl, adjusted pH, polymer).

## 2 Materials and methods

### 2.1 Wastewater treatment plants

Samples of wastewater and blockage were obtained from two CMP wastewater treatment plants in Taiwan, which used similar treatment processes. Besides CMP wastewater, the treatment plant also received effluent from the biological wastewater treatment plant, which makes up about 5% of the total inflow. The wastewater streams were combined in the buffer tank, then flowed to the pH adjustment tank where PACl was dosed, and the pH was adjusted to 8.5 by adding NaOH or $H_2SO_4$. The process followed by rapid mixing in the coagulation tank, slow mixing in the flocculation tank (with anionic polymer addition) and settling in the sedimentation tank. Fig. S1 of Supplementary Materials shows that the discharge pipeline of both plants was blocked by fine particles that created rigid and dehydrated layers. The blockages were partial and cover the inner wall of the discharge pipeline. In Plant B, an intensive sampling was conducted to monitor the changes in turbidity, suspended solids (SS), colloidal Si, soluble Cu, soluble-Al, conductivity, pH, and zeta potential in the field, while the samples were taken from the buffer tank and sedimentation tank (effluent) for 3 wk with 6 h intervals.

### 2.2 SEM/EDX analysis

SEM/EDX analysis was performed on the SS of effluent and the blockage samples collected from the plants. The effluent samples were prefiltered with Whatman Glass Microfiber Filter (GF/D 47 mm). The SS and blockage samples were then dried at room temperature. One subsample of blockage from Plant A was heat-treated at 500 °C for 3 h to evaporate the organic matter. The composition of SS and blockages were characterized by SU8000 SEM, coupled to EDX detector (Hitachi, Japan).

### 2.3 Jar tests

All jar tests were carried out on wastewater collected from the buffer tank of Plant A and Plant B, and the PACl and anionic polymer used in the test were also

form the plant. The jar tests were conducted with a procedure following the operation in the plants, as described below. Firstly, 500-mL plastic vials filled with 200 mL of wastewater and placed on an orbital shaker with an adjustable speed. A predetermined dosage of coagulant was added to the wastewater, and the pH was adjusted using NaOH and $H_2SO_4$ before being shaken at 100 rpm for 3 min. Polymer addition was then followed by mixing at 30 rpm for 15 min, and another 15 min of settlement was performed. Finally, 40 mL of supernatant was taken for water quality analyses and the in-bottle test, while the settled sludge was sampled to analyze the dry weight of the produced sludge. Two batches of jar test were conducted in the study. For the first batch, the polymer dosage was varied (0–2 mg $L^{-1}$) under fixed pH of 8.5. For the second batch, the dosage of polymer was fixed at optimum value determined from the first batch of jar test, however, 40–50 mg $L^{-1}$ of $CuSO_4$ was added to raw wastewater to spike the soluble Cu concentration while pH was adjusted in the range between 8–9.5.

### 2.4 In-bottle test

To simulate the stagnant flow in the discharge pipeline, the supernatant sampled from the jar test was placed in a 50-mL plastic tube and allowed to stand at room temperature. After months, pH and the concentrations of total-Al, soluble-Al, total-Cu, and soluble-Cu were measured. By subtracting the total concentrations of Al or Cu before and after the in-bottle test, the deposited-Al/Cu could be determined. It should be noted that only the supernatants from jar tests with high turbidity in each batch were collected for in-bottle test.

### 2.5 Polynomial response model

In order to establish the relationship between variables, the jar test data were fitted into polynomial response models given by Eq. (3), using the Curve Fitting Toolbox in MATLAB (Mathworks, Natick, MA) software.

$$z = \sum_{i=0}^{n} \sum_{j=0}^{m} p_{ij} x^i y^j \tag{3}$$

In the equation, z is the dependent variable (response); x and y represent the independent variables; n is the polynomial degree of variable x; m is the polynomial degree of variable y; p is the coefficient. Each model was named Polynm, for example, Poly12 represents a surface fitting with the first-degree polynomial model for variable x ($n=1$) and second-degree polynomial for variable y ($m=2$). The best-fitted model was determined by examining the numerical fit and graphical fit.

### 2.6 Analytical methods

Samples were sent to the Instrument Center of National Cheng Kung University for SEM/EDX analysis. The turbidity was measured as nephelometry turbidity units (NTU) using a Laboratory Turbidimeter 2100 N (Hach, USA). Zeta potential was determined using Zetasizer 2000 (Malvern Panalytical, United Kingdom). Conductivity and pH were determined using DS-51 conductivity meter (HORIBA, Japan) and pH/ORP controller PC-310 (SUNTEX, Taiwan). Non-purgeable dissolved organic carbon was determined using the combustion infrared method using a total organic carbon analyzer (TOC-500, Shimadzu, Japan). To analyze the soluble metals (Cu, Ni, and Al) in the sample, the supernatant was prefiltered using 0.22 μm membranes and then analyzed using inductively coupled plasma optical emission spectroscopy (ICP-OES; ULTIMA 2000, HORIBA, Japan). SS and sludge production were measured according to the Standard Methods 2540D and 2540B, respectively [21].

As for the silica analysis, including total-Si and dissolved-Si (filtered by 0.45 μm membrane), was performed as suggested by Bossert et al. [22]: 1 mL of 2.8% KOH was added to the 25-mL samples and followed by 1 h of digestion in the autoclave. Samples for Al and Cu analyses were firstly acidified with $HNO_3$ and $H_2SO_4$ (1:1) and digested at 65 °C for 8 h [23]. After cooling, all samples were filtered through 0.22 μm membranes and then analyzed using ICP-OES to detect the metal concentration.

## 3 Results and discussion

### 3.1 Composition of suspended solid in the effluent and the blockage

To firstly identify the composition of SS in the effluent and the blockage, SEM/EDX analysis was applied, and the results are presented in Table 1 and Fig. S2. Except for C and O, Al (17.5%) was the highest element in the effluent taken from Plant A, whereas Si (24.7%) was dominant in that from Plant B (Table 1). The pipeline blockage in Plant A and B, however, exhibited high Al content, suggesting that most of the operations in both plants were at overdosage of PACl. It was also revealed that a part of the blockage in the pipeline of Plant A was organic, since the percentage of C decreased from 32.5 to 7.0% after 500 °C of heating for 3 h. In addition, the SEM images of both blockages in Fig. S2 were identical to those of high dosage of PACl described by Lin et al. [24] in which the sediments contain many amorphous matters. The results suggested that the blockage was mostly caused by enmeshment of residual particles by amorphous hydroxide precipitate which then formed sweep flocs. Given that the main mechanism at this condition was sweep flocculation that is primarily promoted by colloidal Al

**Table 1** SEM/EDX results of the SS of effluent and blockages

| Samples | Elements (wt%) | | | | | | |
|---|---|---|---|---|---|---|---|
| | C | O | Al | Si | Na | S | Cu |
| *Plant A* | | | | | | | |
| SS of effluent | 45.20 | 25.95 | 17.52 | 6.57 | 2.45 | 2.32 | - |
| Pipeline blockage | 32.47 | 34.38 | 27.60 | 3.70 | 0.65 | 1.20 | - |
| Pipeline blockage (500 °C, 3 h) | 6.95 | 32.99 | 50.22 | 9.85 | - | - | - |
| *Plant B* | | | | | | | |
| SS of effluent | 25.57 | 40.56 | 6.29 | 24.67 | 2.90 | - | - |
| Pipeline blockage | 25.52 | 36.23 | 23.65 | 8.82 | - | - | 5.77 |

species [25], flocs formed by polymeric Al with small and medium size organic matter are colloidal and not easy to precipitate during sedimentation [26]. As higher dosage of PACl was added, more colloidal Al would present in the treated water, leading to Al deposition in the discharge pipeline.

A considerable amount of Si and Cu elements were also found in the blockages from Plant A and/or B, while the SS in the effluents also contained Si. It is assumed that colloidal Si that was unsettled during sedimentation could form deposited Si in the pipeline of effluent, even when PACl was overdosed. In addition, the present of high C portion in both samples indicated the possible bounds of organic with Cu and with Si. The close percentages of Si (8.8%) and Cu (5.8%) in the blockage from Plant B indicate the formation of residual Si–O-Cu bonds that precipitated in the discharge pipeline [27].

### 3.2 Characterization of CMP wastewater in the treatment plant

Samples in Plant B were taken for 3 wk with 6 h intervals to monitor the variations in water qualities, as summarized in Table 2. The influent wastewater contains high turbidity, SS, and soluble Cu with negative zeta potential,

**Table 2** Characterization of the influent and effluent in Plant B

| Parameter | Influent[a] | Effluent[a] | Standard[c] |
|---|---|---|---|
| Turbidity (NTU) | 76–41,100 | 1–159 | - |
| SS (mg L$^{-1}$) | 8–4476 | 0.1–17.3 | 250 |
| Colloidal Si (mg L$^{-1}$) | 7–3876 | 0.1–15 | - |
| Soluble Cu (mg L$^{-1}$) | 0.08–19.06 | 0–0.29 | 1 |
| Soluble Ni (mg L$^{-1}$) | 0–0.59 | 0–0.21 | 0.7 |
| Soluble Al (mg L$^{-1}$) | 0.04–1.29 | 0.07–0.86 | - |
| Conductivity (μS cm$^{-1}$) | 637–5320 | 839–4830 | - |
| pH | 2.6–9.2 | 6.7–8.6 | 5—10 |
| Zeta potential (mV) [b] | -19.4—(-3.8) | -11.7—(3.8) | - |

[a] 76 samples; [b] 48 samples; [c] Permissible effluent limit by Taiwan EPA

whereas the effluent contains low turbidity, SS, and soluble copper with more positive zeta potential. Chemical oxygen demand (COD) concentrations in the influent and effluent were not monitored since they were always below 30 mg L$^{-1}$ according to operational experiences and the occasional sampling, implying that COD in the influent did not participate in the coagulation/flocculation reactions. Soluble Cu and SS levels, the only two subjects that are regulated by Taiwan EPA, were far below the standards despite the high concentrations in the influent. The highest turbidity and soluble Cu recorded during the period were 41,100 NTU and 19.06 mg L$^{-1}$. The results implied that coagulation-flocculation using PACl as coagulant and anionic polymer as flocculant at pH 8.5 could effectively remove turbidity and Cu from the wastewater. The soluble Al and conductivity in the influent and effluent remained relatively the same. The pH of influent was mostly neutral, while pH of the effluent was about 8. A slight drop of pH, from 8.5 during coagulation to about 8 in the effluent, indicates the hydrolysis of Al during the process [9]. The values of zeta potential were generally negative in the influent, which indicates the presence of negatively charged particles, i.e., colloidal Si, SS in wastewater. It was also revealed that the SS and colloidal Si were positively correlated to turbidity with a coefficient of determination ($R^2$) of over 0.87, as shown in Fig. 1. It indicates that the source of turbidity and SS in the wastewater was potentially contributed by colloidal Si, which was in agreement with previous study by Kuan and Hu [2]. Silica particle is anionic at pH above 2 and would dissolve in water by forming silicic acid and silicate ions at pH above 7 [28]. The zeta potential values were close to zero in the effluent, indicating charge neutralization by PACl during coagulation and flocculation process, however, some were still negative despite the residual turbidity being less than 40 NTU. Aside from the residual colloidal Si, the negative zeta potential in the effluent was presumably caused by residual organic matter, namely anionic polymer. Saxena et al. [29] suggested

Praptiwi *et al. Sustainable Environment Research*    (2022) 32:37
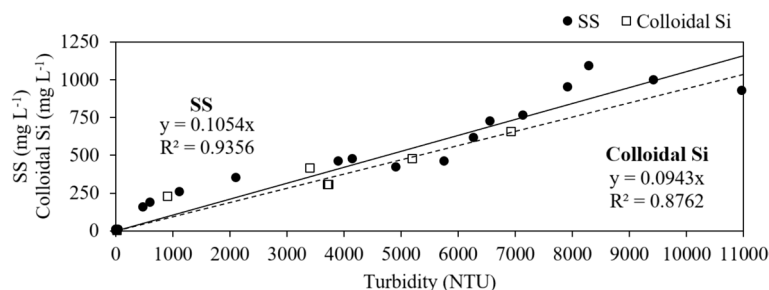
Page 5 of 12



**Fig. 1** SS and colloidal Si as a function of turbidity in the raw wastewater (pH 6.6–9.34)

that the presence of total organic carbon as low as 2 mg $L^{-1}$ could exhibit zeta potential around -15 mV, while the remaining organic matter could contribute to the occurrence of the blockage as part of the C in blockage was mainly organic (Table 1).

### 3.3 Factors affecting PACl dosage

#### 3.3.1 Effects of anionic polymeron PACl dosage

Figure 2 presents the result of the first batch of the jar test with the variation in the polymer dosage during flocculation. In all cases, the residual turbidity in the process with polymer addition was lower than those without polymer, and while the addition of anionic polymer could improve turbidity removal, as shown in Fig. 2a and c. Moreover, the polymer also lowered the required

PACl for low residual turbidity. PACl dosage of 150 mg $L^{-1}$ was required to reach residual turbidity of around 30 NTU without the addition of polymer, while only 10 and 50 mg $L^{-1}$ of PACl was required for wastewaters with low turbidity and high turbidity, respectively. Polymer addition would increase floc size and density and improve turbidity removal and floc settleability [30]. The higher dosage of PACl needed for the wastewater with low turbidity might be due to the limitation of interparticle collision, as the amount of colloidal Si was much lower than that with high turbidity. Polymer dosage of 2 mg $L^{-1}$ did not further improve the turbidity removal, consequently, 1 mg $L^{-1}$ was considered to be the optimum dosage in the following test. When the excess polymer is added, the unoccupied polymer would remain
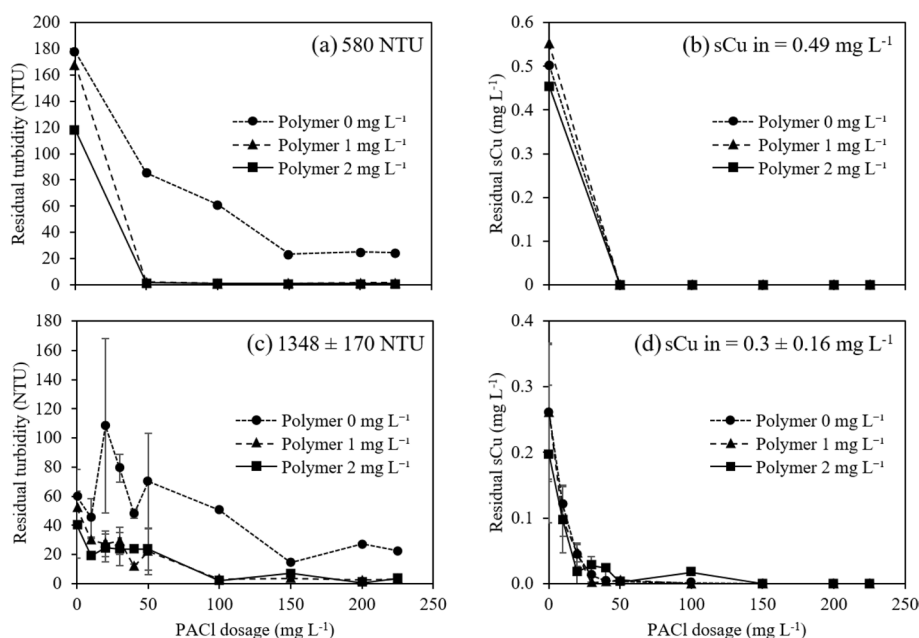


**Fig. 2** Effect of polymer dosage on residual turbidity and soluble Cu at low initial turbidity of 580 NTU (**a**, **b**) and high initial turbidity of 1348 NTU (**c**, **d**). (Experimental conditions: PACl dosage 0, 10, 20, 30, 40, 50, 100, 150, 200, and 225 mg $L^{-1}$; polymer dosage 0, 1, and 2 mg $L.^{-1}$; pH adjusted to 8.5)

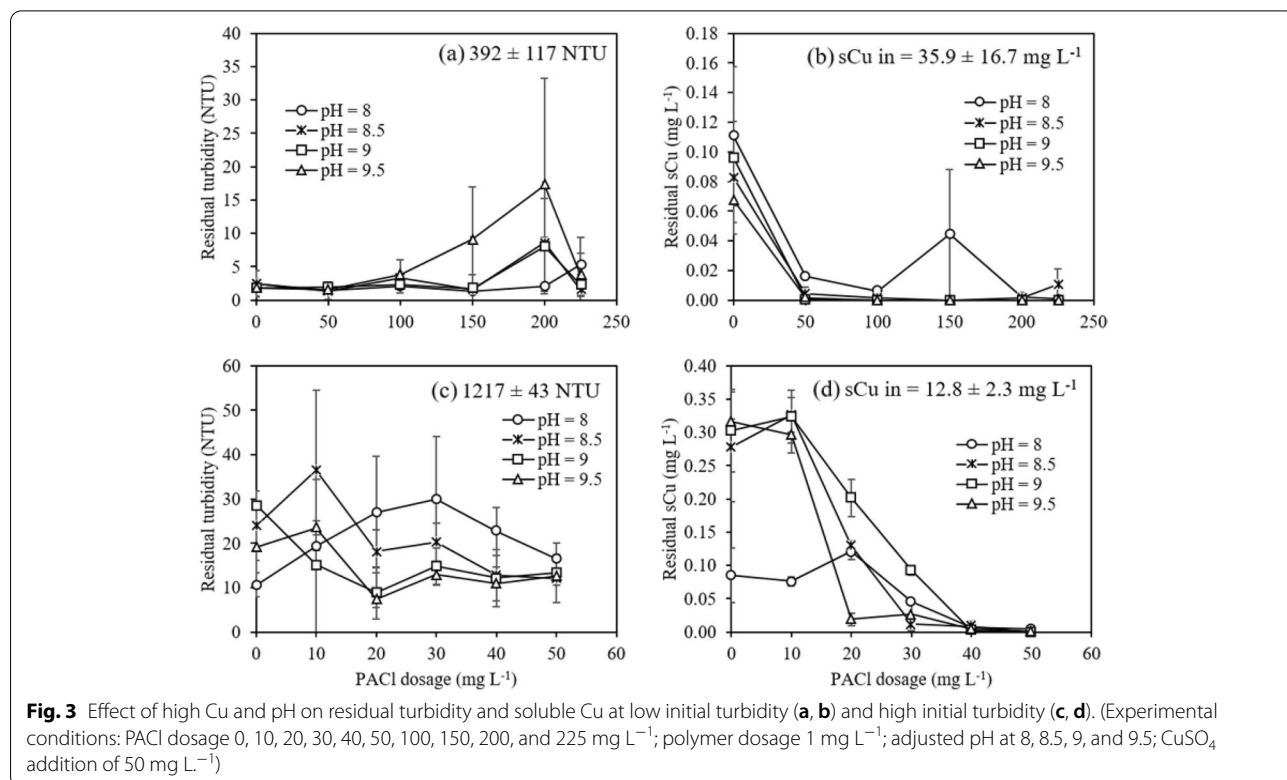free in the water due to the lack of available adsorption and bridging sites [31].

Under the optimum polymer dosage, most turbidity could be removed, from 580 to 168 NTU (71%) and around 1350 to 60 NTU (95%), with only pH adjustment to 8.5 during coagulation. In this case, the coagulation-flocculation persumably occurred by double-layer compression due to the adsorption of positively charged ions on the Stern layer of silica [32], while Iler [28] also suggested that the adsorbed monovalent and divalent metal cations could bridge the silica particles and promote coagulation. The turbidity removal with only pH adjustment (no PACl and polymer addtion) may also be attributed to the increase of silica solubility at basic pH due to the dissolution of silica and complexation reaction with metals and organic matter [33].

Anionic polymer did not have a significant effect on soluble Cu removal regardless of the initial turbidity (Fig. 2b and d). The soluble Cu was removed when a higher dosage of PACl was added. The colloidal Al species (as $Al(OH)_3$) could adsorb $Cu^{2+}$ with a capacity of 370 mg $g^{-1}$ [34]. In addition, Lopez-Maldonado et al. [35] suggested a removal mechanism of the metal cation-organic complex via simultaneous adsorption of metal cation site to anionic polymer and organic matter site to polymeric coagulant. Although both positively and negatively charged polymers were present in the system, it seems that the first was the dominant one.

### 3.3.2 *Effect of Cu and pH on PACldosage*

With higher Cu concentrations in the second batch of jar test, results shows that the residual turbidity was mostly below 40 NTU no matter the initial turbidity levels or the pH ranges between 8 to 9.5, as shown in Fig. 3. Wastewater with high turbidity, however, required higher dosage of PACl to achieve low residual turbisity, while higher dosages of PACl (150–200 mg $L^{-1}$) exhibited higher residual turbidity under high pH in the wastewater with low turbidity due probably to the restabilization of particles. In the test of low turbidity wastewater with the pH of 8.5, low residual turbidity could be achieved even when PACl was not added (Fig. 3a), which was different with that without Cu addition (Fig. 2a). Furthermore, the SEM/EDX results showed that there is lower portion of Al (23.7%) in the blockages for Plant B, in which Cu deposition occurred. The existence of Cu ions in coagulation-flocculation could lead to lower PACl dosage due to the synergistic effect through the interactions among coagulants, colloids, organics and Cu ions or Cu hydroxide ($Cu(OH)_2$) formed at higher pHs. The precipitated $Cu(OH)_2$ might increase the number of particles and compensate for the lack of quantity of particles, and it could also act



**Fig. 3** Effect of high Cu and pH on residual turbidity and soluble Cu at low initial turbidity (**a**, **b**) and high initial turbidity (**c**, **d**). (Experimental conditions: PACl dosage 0, 10, 20, 30, 40, 50, 100, 150, 200, and 225 mg $L^{-1}$; polymer dosage 1 mg $L^{-1}$; adjusted pH at 8, 8.5, 9, and 9.5; $CuSO_4$ addition of 50 mg $L^{-1}$)

Praptiwi *et al. Sustainable Environment Research*      (2022) 32:37

Page 7 of 12

as an electrostatic bridge for colloidal Si [30] although the mechanism may only occur at pH below 9 where $Cu(OH)_2$ is positively charged [36]. In addition, the presence of 1 mg $L^{-1}$ anionic polymer could facilitate the formation of particle-binding cationic bridges via adsorbed $Cu^{2+}$ [37]. Similarly, the residual turbidity of the wastewater with high turbidity could be reduced to under 40 NTU even without adding PACl (Fig. 3c), as 10 mg $L^{-1}$ of PACl was required for that without Cu supplement (Fig. 2c). The lower requirement of PACl might be because of its slightly lower initial turbidity, as higher PACl dosage was needed to remove more colloidal Si as turbidity. Hence, it could be deducted that the optimum PACl dosage for wastewater with low initial turbidity was dependent on the initial soluble Cu in which higher initial soluble Cu required lower PACl dosage, and it was more dependent on initial turbidity for wastewater with high initial turbidity.

As for the Cu removal, it could be observed that higher pH exhibited lower residual soluble Cu although the effect was insignificant in wastewater with high initial turbidity (Fig. 3b and d), which was presumably due to the shift of Cu solubility by reacting with silicic acid [33]. The initial soluble Cu in wastewater with high initial turbidity was lower than that with low residual turbidity, although almost the same amount of Cu was added. It implied that most Cu ions were adsorbed on colloidal Si in the wastewater with higher turbidity. The residual soluble Cu could be removed to less than 0.4 mg $L^{-1}$ with no PACl addition regardless of the initial turbidity, indicating that the soluble Cu was removed by Cu precipitation by forming $Cu(OH)_2$ at pH above 8 [34] and could meet the standard set by Taiwan EPA. Based on the results, the operation could focus on adjusting the PACl dosage for turbidity removal with the assurance of low residual soluble Cu because the main mechanism for soluble Cu removal was adsorption by colloidal Si and Cu precipitation.

### 3.4 Effect of PACl and anionic polymer on Al and Cu deposition

To simulate the deposition that happened in the discharge pipeline which might lead to the blockage, in-bottle test was conducted after the jar tests in which the supernatants were stagnated for around 10 months. The total residual Al and Cu before and after the stagnation of the first batch of jar test (under different polymer dosages) are summarized in Fig. 4. Although the residual turbidity was decreased as PACl dosage increased, the residual Al was increased (Fig. 4a). This might be due to the small size of Al particulate in the treated water, hence it was not measured as turbidity during the analysis. Yao et al. [38] revealed that small particles (less

than 5 μm) could cause the light intensity to be equally scattered in all directions during the turbidity measurement and interfere the result. Nevertheless, the result shows that overdosing PACl would increase the residual Al. At all conditions, the total residual Al after stagnation was constant at around 1.5 mg $L^{-1}$, accordingly, the deposited Al followed the same trend as total residual Al before stagnation. Zhang et al. [39] reported that polymeric Al species could deposit due to self-aggregation of $Al_{13}(AlO_4Al_{12}(OH)_{24}(H_2O)_{12}{}^{7+})$ at high pH which increased its molecular weight. As pH and PACl dosage increased, the OH group of $Al_{13}$ had a weaker charge and an increased affinity to cations in a coiled structure [24]. In addition, the residual soluble Al was also reduced after the stagnation condition, indicating the deposition of soluble Al onto organic matter [26]. It was also observed that the pH of the supernatants was reduced during stagnation, as Table S1 summarized, implying the hydrolysis of residual monomeric Al and polymeric Al.

In the case of Cu, the total residual-Cu before stagnation decreased as PACl dosage increased, and the total residual-Cu concentration after stagnation was relatively stable at around 0.25 mg $L^{-1}$. As more PACl added, the Cu ions would be absorbed by the formed flocs during coagulation-flocculation, hence less residual Cu. In summary, the addition of polymer increased the deposited Al and reduced the deposited Cu due to their reaction with anionic polymer, therefore polymer dosage needs to be optimized in order to minimize the deposit.

As for the second batch (under different pH during coagulation), the total residual Al and Cu before and after the stagnation are shown in Fig. 5. Results indicate that pH would increase Al deposition, more significantly at over dosage of PACl. In addition, the residual Al after stagnation condition was slightly increasing as the PACl dosage increase. The increase of residual Al might be caused by a build-up of residual monomeric Al (as $Al(OH)^{4-}$), since the proportion of polymeric Al in PACl did not change much with increase in pH [40]. The pH of the supernatant during stagnation was also reduced (Table S2) although the reduction was less than those in the first batch (Table S1), implying the monomeric Al was hydrolyzed and deposited. Higher residual Al levels were observed after stagnation when adjusting pH as high as 9.5 during coagulation, indicating some flocs were formed by the residual soluble Al and organic matters in the supernatant. The effect of pH during coagulation on the deposition of residual Cu was not significant. In general, deposited Cu was the lowest with no PACl addition and increased at PACl dosage of 10 mg $L^{-1}$. It could be possible that the residual monomeric Al and polymeric Al bounded to Cu and form bigger flocs which apt to deposit.
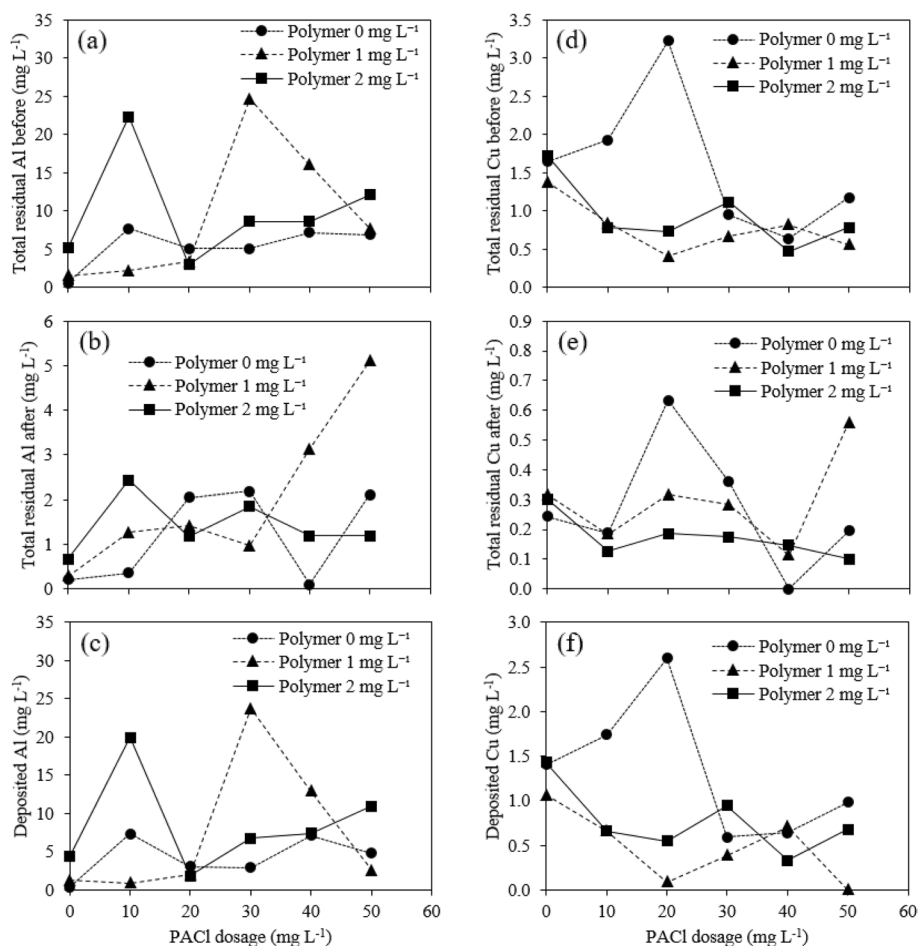
Praptiwi *et al. Sustainable Environment Research*      (2022) 32:37

Page 8 of 12



**Fig. 4** Effect of polymer on residual Al deposition (**a**, **b**, **c**) and residual Cu deposition (**d**, **e**, **f**). (Experimental conditions: Initial turbidity 1140 NTU; PACl dosage 0, 10, 20, 30, 40, and 50 mg L$^{-1}$; polymer dosage 0, 1, and 2 mg L.$^{-1}$; adjusted pH at 8.5)

### 3.5 The deposition in discharge pipeline

According to the results obtained in jar tests, the sedimentation in the discharge pipeline could occur when the addition of PACl was not optimized. First of all, although adding PACl reduces residual turbidity, overdosed PACl can result in the excess monomeric Al and polymeric Al in the treated wastewater (Fig. 4a). The residual Al, after hydrolysis, may deposit with residual organic matters, anionic polymer and/or Cu during stagnation, as shown in Table 2 that Al was the main element in the pipeline blockage in both plants along with organics (C and O) and/or Cu. Adding appropriate concentration of polymer, such as 1 mg L$^{-1}$ in the study, could improve turbidity removal and produce the least Al and Cu deposits, while 2 mg L$^{-1}$ of polymer addition only deposited the excess polymer. High soluble Cu in the wastewater reduces PACl required by forming copper hydroxides to increase precipitates and act as an electrostatic bridge, while residual

Cu deposits with Al during stagnation (Figs. 4 and 5). Controlling pH above 8.5 during coagulation aggravates the deposit of residual Al due to the increase of monomeric Al, which forms more complex with residual organic matter. Secondly, in the case with absent PACl, residual Cu turns to adsorb onto colloidal Si and its aggregation with other flocs could also deposit in the pipeline, as part of Cu was still deposit after stagnation for 10 months (Figs. 4f and 5f). In summary, it was highly suggested to operate the coagulation-flocculation process at the optimum dosage of the PACl, which was dependent on the initial soluble Cu for wastewater with low initial turbidity and on the initial turbidity for wastewater with high initial turbidity. Sensors and automatic controlling system for the dosage of PACl, in the case, are essential to prevent blockage in the discharge pipeline, while predetermining the adjusted pH and anionic polymer dosage for the process was also necessary.
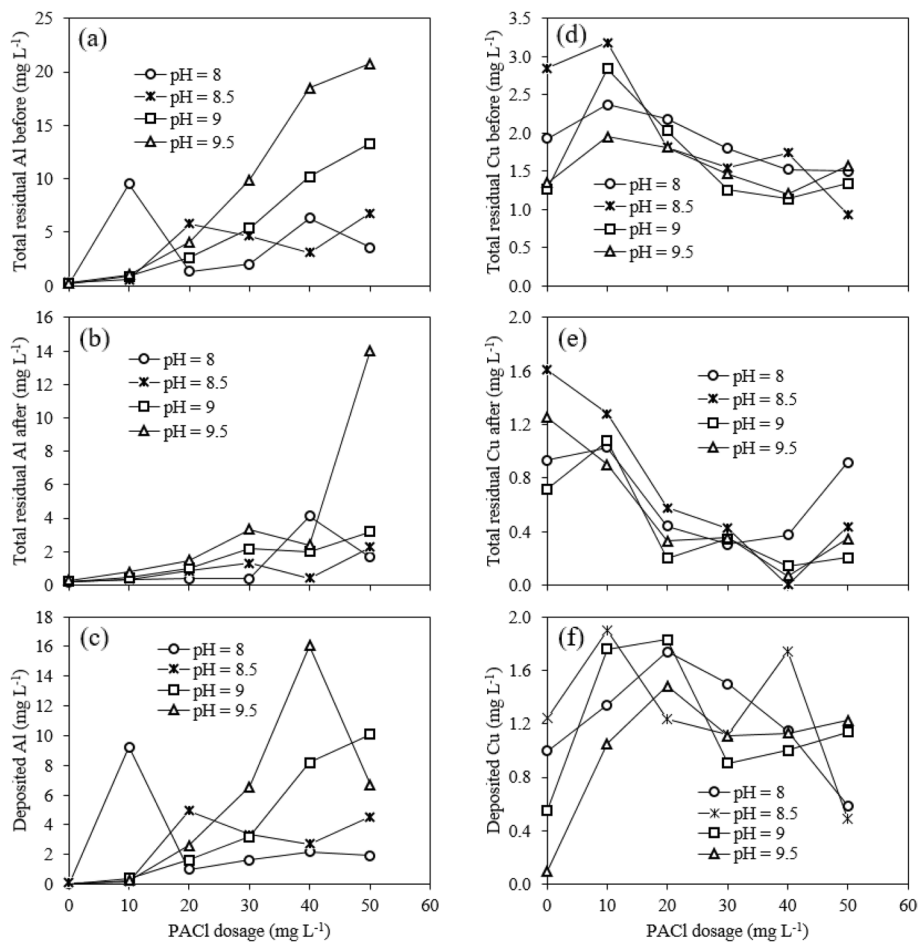
Praptiwi *et al. Sustainable Environment Research*      (2022) 32:37

Page 9 of 12



**Fig. 5** Effect of high Cu and pH on residual Al deposition (**a**, **b**, **c**) and residual Cu deposition (**d**, **e**, **f**). (Experimental conditions: Initial turbidity 1260 NTU; PACl dosage 0, 10, 20, 30, 40, and 50 mg $L^{-1}$; polymer dosage 0, 1 mg $L^{-1}$; adjusted pH at 8, 8.5, 9, and 9.5; CuSO$_4$ addition of 50 mg $L.^{-1}$)

### 3.6 Surface fitting regression for optimized PACl dosage

To figure out the optimum dosage of PACl, the obtained data from jar tests with pH adjusted at 8.5 and polymer dosage of 1 mg $L^{-1}$ were fitted into polynomial response models. It is known previously that PACl dosage of wastewater with low initial turbidity (< 1000 NTU) is more dependent on the initial soluble Cu concentration while that of wastewater with high initial turbidity ($\geq$ 1000 NTU) is based on initial turbidity. In the case, initial soluble Cu and initial turbidity were used respectively according to the initial turbidity as the independent variables together with the PACl dosage, while residual turbidity is the dependent variable. For the wastewater with low turbidity, model with degree of 1 on both initial soluble Cu and PACl dosage (Poly11) performed the low sum squared error and the highest adjusted coefficient of determination ($R^2 = 0.79$). Models with degree of 1 on initial turbidity and degree of 2 on PACl dosage (Poly12),

on the other hand, were the best to describe the residual turbidity for wastewater with high turbidity. Accordingly, the optimal PACl dosage could be calculated, as Fig. 6 depicted. Specifically, for wastewater with initial turbidity of 1000 to 2200 NTU, the optimum PACl dosage was recommended to be 0 mg $L^{-1}$ (Fig. 6a), and it increased proportionately as initial turbidity increased. If the initial turbidity in the wastewater is below 1000 NTU, the control should be switched to initial soluble Cu concentration (Fig. 6b), while the optimum PACl dosage was determined to be 50 mg $L^{-1}$ for soluble Cu below 0.4 mg $L^{-1}$ and it decreased exponentially with soluble Cu concentration to 0 mg $L^{-1}$ when soluble Cu above 18.8 mg $L^{-1}$.

## 4 Conclusions

In this study, SEM/EDX analysis, jar test, and in-bottle test were used to link the pipeline blockages to the coagulation-flocculation process in the CMP wastewater
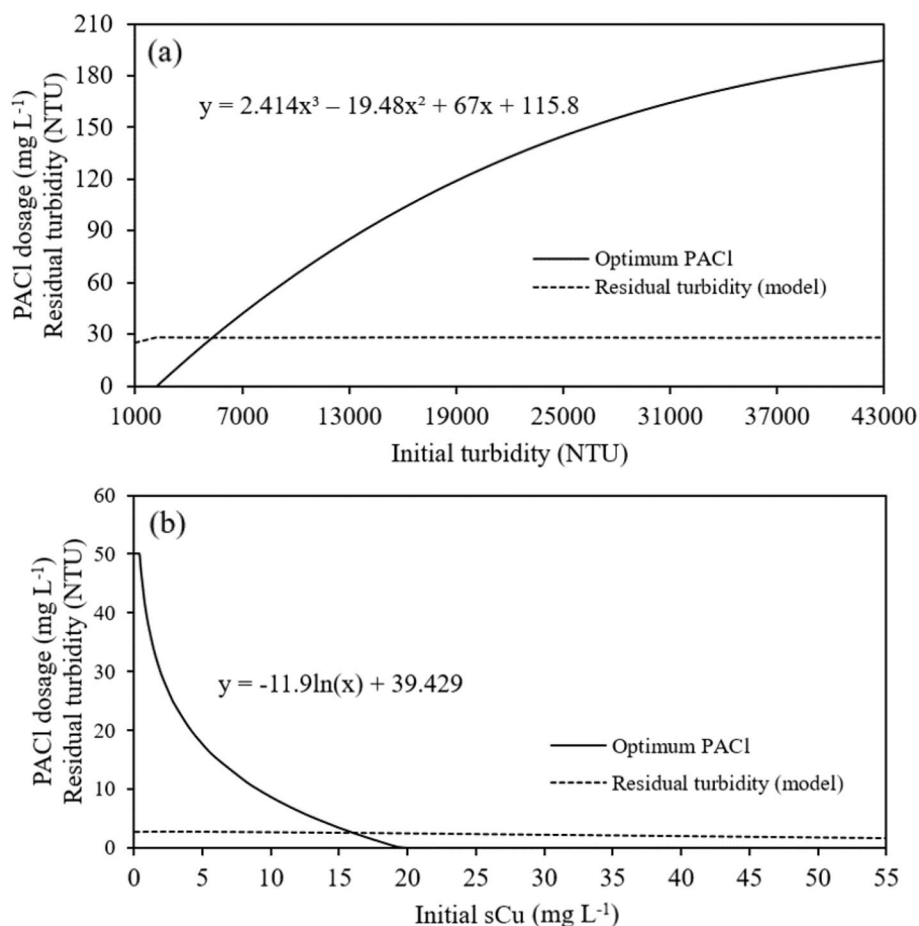
**Fig. 6** Proposed optimum PACl dosage for (**a**) high initial turbidity water and (**b**) low initial turbidity water

treatment plant. Results indicated that blockages were mainly caused by residual polymeric Al bound to organic matter, as well as the sedimentation of residual Cu and the turbidity (primarily colloidal Si). Therefore, the PACl dosage should be increased carefully according to the increasing initial turbidity and prevent residual Al in the effluent, while the addition of PACl could be reduced with increasing Cu concentration when initial turbidity is low and count on its self-sedimentation. It was also revealed that excess polymer addition resulted in higher Al and Cu deposition due to residual metal-anionic polymer flocs, and pH adjustment over 9 could lead to deposition of Al by forming complex of residual monomeric Al, organic matter, and colloidal Si. In sum, operation at the optimum PACl dosage, polymer dosage, and pH would minimize the blockage occurrence in the pipeline because the residual Al, Cu, and polymer would be reduced. Hence, it is suggested to use automatic control in adjusting the PACl dosage for the prevention of the blockage.

## Supplementary Information

The online version contains supplementary material available at https://doi.org/10.1186/s42834-022-00147-6.

**Additional file 1: Fig. S1.** Photograph of blockages in the discharge pipeline of Plant A (left) and Plant B (right). **Fig. S2.** SEM image of pipeline blockage of Plant A (left) and Plant B (right). **Table S1.** pH reduction during stagnation (polymer variation; from pH = 8.5). **Table S2.** pH reduction after stagnation condition (pH variation; from the adjusted pH).

## Authors' contributions

This study was conceptualized and designed by Liang-Ming Whang and Hai-Hsuan Cheng. Experiments and data collection were conducted by Rosalina Eka Praptiwi and Jyun-Cyuan Syu. The manuscript was written by Rosalina Eka Praptiwi and Hai-Hsuan Cheng, and was revised and approved by Liang-Ming Whang. The author(s) read and approved the final manuscript.

Praptiwi *et al. Sustainable Environment Research*    (2022) 32:37

Page 11 of 12

## Availability of data and materials
The datasets generated are available from the corresponding author upon reasonable request.

## Declarations

### Competing interests
The authors declare that they have no known competing financial interests or personal relationships that could have appeared to influence the work reported in this paper.

### Author details
[1]Department of Environmental Engineering, National Cheng Kung University, Tainan 701, Taiwan. [2]Advanced Semiconductor Engineering Group, Kaohsiung 811, Taiwan. [3]Sustainable Environment Research Laboratory, National Cheng Kung University, Tainan 701, Taiwan.

## References
1. Noor IE, Coenen J, Martin A, Dahl O. Performance assessment of chemical mechanical planarization wastewater treatment in nano-electronics industries using membrane distillation. Sep Purif Technol. 2020;235:116201.
2. Kuan WH, Hu CY. Chemical evidences for the optimal coagulant dosage and pH adjustment of silica removal from chemical mechanical polishing (CMP) wastewater. Colloid Surface A. 2009;342:1–7.
3. Lai CL, Lin SH. Treatment of chemical mechanical polishing wastewater by electrocoagulation: system performances and sludge settling characteristics. Chemosphere. 2004;54:235–42.
4. Yang GCC, Tsai CM. Preparation of carbon fibers/carbon/alumina tubular composite membranes and their applications in treating Cu-CMP wastewater by a novel electrochemical process. J Membrane Sci. 2008;321:232–9.
5. Makhviladze TM, Sarychev ME. The model of the process of the chemical mechanical polishing of the copper metallization, based on the formation of the passivation layer. Russ Microelectron. 2018;47:344–53.
6. Chuang SH, Chang TC, Ouyang CF, Leu JM. Colloidal silica removal in coagulation processes for wastewater reuse in a high-tech industrial park. Water Sci Technol. 2007;55:187–95.
7. Den W, Huang CP. Electrocoagulation for removal of silica nano-particles from chemical-mechanical-planarization wastewater. Colloid Surface A. 2005;254:81–9.
8. Wu XH, Ge XP, Wang DS, Tang HX. Distinct coagulation mechanism and model between alum and high $Al_{13}$-PACl. Colloid Surface A. 2007;305:89-96.
9. Wei N, Zhang ZG, Liu D, Wu Y, Wang J, Wang QH. Coagulation behavior of polyaluminum chloride: effects of pH and coagulant dosage. Chinese J Chem Eng. 2015;23:1041–6.
10. He WP, Xie ZL, Lu WJ, Huang ML, Ma JW. Comparative analysis on floc growth behaviors during ballasted flocculation by using aluminum sulphate (AS) and polyaluminum chloride (PACl) as coagulants. Sep Purif Technol. 2019;213:176–85.
11. Chen ZY, Fan B, Peng XJ, Zhang ZG, Fan JH, Luan ZK. Evaluation of $Al_{30}$ polynuclear species in polyaluminum solutions as coagulant for water treatment. Chemosphere. 2006;64:912–8.
12. Wu Z, Zhang X, Zhou CJ, Pang JL, Zhang PY. A comparative study on the characteristics and coagulation mechanism of PAC-$Al_{13}$ and PAC-$Al_{30}$. RSC Adv. 2016;6:108369–74.
13. Tang HX, Xiao F, Wang DS. Speciation, stability, and coagulation mechanisms of hydroxyl aluminum clusters formed by PACl and alum: a critical review. Adv Colloid Interfac. 2015;226:78–85.
14. Li RH, Gao BY, Sun JZ, Yue QY. Coagulation behavior of kaolin-anionic surfactant simulative wastewater by polyaluminum chloride-polymer dual coagulants. Environ Sci Pollut R. 2018;25:7382–90.
15. Costello JJ. Postprecipitation in distribution systems. J Am Water Works Ass. 1984;76:46–9.
16. Jafari R, Razvarz S, Vargas-Jarillo C, Gegov A. Blockage detection in pipeline based on the extended Kalman filter observer. Electronics-Switz. 2020;9:91.
17. Chilarescu IC, Berevoianu C, Sandu M, Racoviteanu G. Automatic determination of coagulation-flocculation reagents dose. In: Hahn HH, Hoffmann E, Ødegaard H, editors. Chemical water and wastewater treatment V. Berlin and Heidelberg: Springer; 1998, p. 71–81.
18. Huang CP, Liu CB. Automatic control for chemical dosing in laboratory-scale coagulation process by using an optical monitor. Water Res. 1996;30:1924–9.
19. Mortadi A, Chahid E, Elmelouky A, Chahbi M, El Ghyati N, Zaim S, et al. Complex electrical conductivity as a new technique to monitor the coagulation-flocculation processes in the wastewater treatment of the textile Industry. Water Resour Ind. 2020;24:100130.
20. Rawlings JO, Pantula SG, Dickey DA. Applied regression analysis: a research tool. 2nd ed. New York: Springer; 1998.
21. APHA, AWWA, WEF. Standard methods for the examination of water and wastewater. 22nd ed. Washington, DC, Denver, Alexandria: American Public Health Association, American Water Works Association, and Water Environment Federation; 2012.
22. Bossert D, Urban DA, Maceroni M, Ackermann-Hirschi L, Haeni L, Yajan P, et al. A hydrofluoric acid-free method to dissolve and quantify silica nanoparticles in aqueous and solid matrices. Sci Rep-UK. 2019;9:7938.
23. He YT, Ziemkiewicz PF. Bias in determining aluminum concentrations: comparison of digestion methods and implications on Al management. Chemosphere. 2016;159:570–6.
24. Lin JL, Huang CP, Chin CJM, Pan JR. Coagulation dynamics of fractal flocs induced by enmeshment and electrostatic patch mechanisms. Water Res. 2008;42:4457–66.
25. Ghernaout D, Ghernaout B. Sweep flocculation as a second form of charge neutralisation–a review. Desalin Water Treat. 2012;44:15–28.
26. Yan MQ, Wang DS, Ni JR, Qu JH, Chow CWK, Liu HL. Mechanism of natural organic matter removal by polyaluminum chloride: effect of coagulant particle size and hydrolysis kinetics. Water Res. 2008;42:3361–70.
27. Zhu WJ, Wang JX, Wu D, Li XT, Luo YM, Han CY, et al. Investigating the heavy metal adsorption of mesoporous silica materials prepared by microwave synthesis. Nanoscale Res Lett. 2017;12:323.
28. Iler RK. The chemistry of silica: solubility, polymerization, colloid and surface properties and biochemistry of silica. New York: Wiley-Interscience; 1979.
29. Saxena K, Brighu U, Choudhary A. Coagulation of humic acid and kaolin at alkaline pH: complex mechanisms and effect of fluctuating organics and turbidity. J Water Process Eng. 2019;31:100875.
30. Bache DH, Gregory R. Flocs in water treatment. London: IWA publishing; 2007.
31. Choy SY, Prasad KMN, Wu TY, Ramanan RN. A review on common vegetables and legumes as promising plant-based natural coagulants in water clarification. Int J Environ Sci Te. 2015;12:367–90.
32. Trefalt G, Behrens SH, Borkovec M. Charge regulation in the electrical double layer: ion adsorption and surface interactions. Langmuir. 2016;32:380–400.
33. Mizutani T, Fukushima Y, Kamigaito O. Mechanism of the copolymerization of silicic acid and metal ions in aqueous media. B Chem Soc Jpn. 1990;63:618–9.
34. Huang CH, Shen SY, Dong CD, Kumar M, Chang JH. Removal mechanism and effective current of electrocoagulation for treating wastewater containing Ni(II), Cu(II), and Cr(VI). Water-Sui. 2020;12:2614.
35. Lopez-Maldonado EA, Oropeza-Guzman MT, Jurado-Baizaval JL, Ochoa-Teran A. Coagulation-flocculation mechanisms in wastewater treatment plants through zeta potential measurements. J Hazard Mater. 2014;279:1–10.
36. Kosmulski M. Compilation of PZC and IEP of sparingly soluble metal oxides and hydroxides from literature. Adv Colloid Interfac. 2009;152:14–25.

Praptiwi *et al. Sustainable Environment Research*     *(2022) 32:37*

Page 12 of 12

37. Lee BJ, Schlautman MA, Toorman E, Fettweis M. Competition between kaolinite flocculation and stabilization in divalent cation solutions dosed with anionic polyacrylamides. Water Res. 2012;46:5696–706.

38. Yao M, Nan J, Chen T. Effect of particle size distribution on turbidity under various water quality levels during flocculation processes. Desalination. 2014;354:116–24.

39. Zhang Y, Shi BY, Zhao YY, Yan MQ, Lytle DA, Wang DS. Deposition behavior of residual aluminum in drinking water distribution system: effect of aluminum speciation. J Environ Sci-China. 2016;42:142–51.

40. Wang D, Sun W, Xu Y, Tang H, Gregory J. Speciation stability of inorganic polymer flocculant–PACl. Colloids and Surfaces A: Physicochemical and Engineering Aspects 2004;243(1-3):1-10.

## Publisher's Note